32nd URSI GASS, Montreal, 19-26 August 2017

# Alternative Implementations of Small All-Platform UHF RFID Transponders

K. Jaakkola
VTT Technical Research Centre of Finland Ltd, Espoo, FI-02044 VTT, Finland, http://www.vtt.fi/en

## Abstract

Analysis and practical implementations of small all-platform UHF RFID transponders are presented. Four prototypes that are combinations of two topologies of integrated impedance matching circuits and two fabrication methods are introduced. With printed circuit board (PCB) technology that is the first of the fabrication methods, prototypes with two and three metal layers are presented. Measurements of the prototypes showed good consistency with the simulation results, demonstrating the effects the different implementation methods have on the transponder performance. The results show that small but efficient transponders can be implemented with various techniques.

## 1. Introduction

The smallest of UHF RFID tags are often based on coupling via inductive near field. As even very low radiation efficiency of the tag antenna greatly improves the read range when compared to that achieved with near field coupling [1], implementing a radiating structure, even with low radiation efficiency, around the microchip is worthwhile in many applications, bringing the read range benefit of UHF RFID technology into action. This presentation concentrates on practical implementation of very small UHF RFID tags, the coupling of which is based on radiating far field. The definition of small here is the largest dimension of the transponder being less than one tenth of a wavelength that is less than 35 mm for a UHF RFID transponder for the European market. The transponders studied and presented are all-platform solutions that work both on dielectric and conductive platforms. Fabrication issues of such tags are also addressed by implementing prototypes with different methods.

## 2. Theory

Implementing a minimum-sized far-field transponder is about packing an efficient radiator, a microchip and structures needed for impedance matching in the constrained space as efficiently as possible. In practice, the size specification of a small transponder is typically defined by a particular application and the design process is about exploiting the given volume.

For every radiating structure that is small compared to the wavelength, regardless whether it is an electric or a magnetic dipole, its intrinsic radiation resistance is very small compared to the input resistance of the microchip. Therefore, in order to maximize the read range, an impedance matching circuitry is needed between the radiator and the microchip. To keep the fabrication costs low, this circuitry has to be an integrated part of the antenna.

As an all-platform tag is targeted, a small loop, the magnetic flux of which is parallel to the mounting platform, is used as a radiator [2, 3]. Figure 1 shows alternative equivalent circuits for matching such a radiator, modelled by resistance $R_a$ and series inductance $L_a$, to the impedance of a typical microchip, modelled by the parallel connection of resistance $R_c$ and capacitance $C_c$. The matching network consists of series capacitance $C_s$ and parallel capacitance $C_p$.

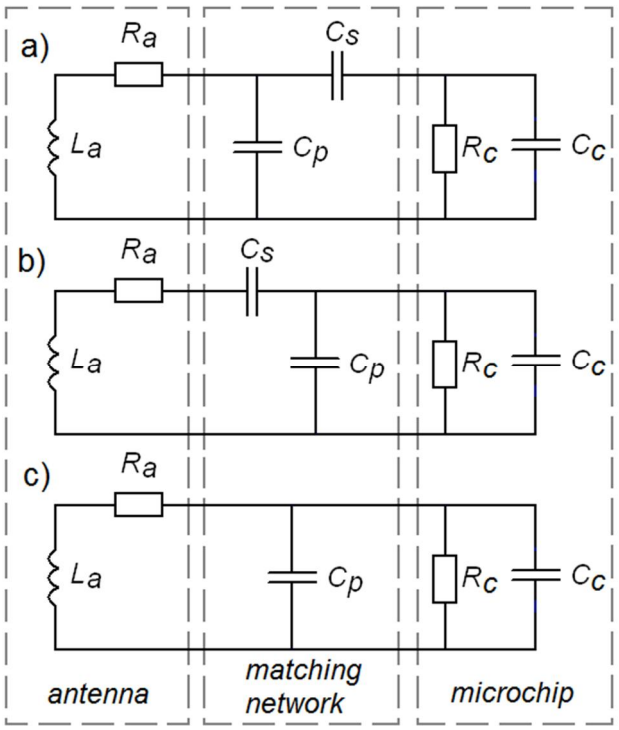


**Figure 1.** Equivalent circuits of a small UHF RFID tag, comprising a small loop antenna, a matching network and a microchip. a), b) and c) represent three alternative implementations of the matching network.

In most of the practical cases with a small loop antenna and the impedance of a typical commercial microchip, both a) and b) can be used for conjugate impedance match. However, alternative a) is often more favorable as it gives smaller capacitance values that are in most cases easier to implement. In some cases, larger capacitances and thus alternative b) may be beneficial as bigger capacitance values may, in certain fabrication processes, also mean smaller relative variation of capacitance and thus smaller variation of center frequency. The alternative c) uses only a parallel capacitor and consequently, it rarely provides conjugate impedance match. However, sometimes, due to limited space, constraints of the fabrication process or if a low-Q antenna is targeted e.g. because of its broader bandwidth, the alternative c) may also be a viable option.

## 3. Transponder prototypes

Four types of transponder prototypes were fabricated. The transponders, shown in Figure 2 and numbered from 1) to 4), are realizations of the equivalent circuits of Figure 1 and are implemented with different fabrication methods.

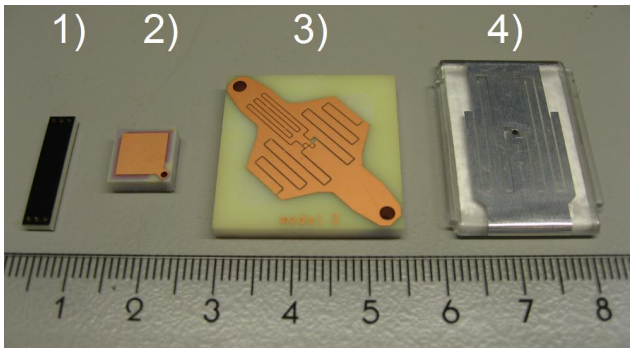


**Figure 2.** Fabricated transponder prototypes 1) – 4).

Prototype 1) is based on the equivalent circuit a) and is fabricated on printed circuit board with three metal layers and two dielectric layers between them. This structure enables the implementation of planar capacitors. The outer dimensions of this transponder are 18 mm * 4 mm * 2 mm. [4]

Prototype 2), 9 mm * 9 mm * 3.3 mm in dimensions, is based on a similar PCB fabrication technology as 1), but uses the simple matching network of type c). The vias connecting the metal layers are positioned in corners so that the radiating loop is in the diagonal direction, which maximizes the cross section area of the loop. The exploded view of prototypes 1) and 2) is shown in Figures 3 and 4 that expose the metal layers I), III) and VI) and the dielectric layers II) and V). The microchip, shown as black on the metal layer III), is embedded inside the substrate [5]. Vias IV a) connect the top and bottom metal layers for type 1) and all three layers for type 2). Vias IV b) connect the mid and bottom metal layers. Capacitors $C_s$ and $C_p$ are thus formed between layers I) and III) for type 1) as $C_p$ is formed between the respective layers for type 2). The dielectric substrate of these transponders is experimental low-loss laminate for high-frequency applications. Its relative permittivity $\varepsilon_r$ is 3.65 and loss tangent $tan(\delta)$ is 0.0035, both measured at 1 GHz. E.g. RO4350B by Rogers Corporation has very similar properties [6].

Prototype 3), 25 mm * 25 mm * 3 mm in dimensions, is also made on PCB using the same materials and has the matching network of type a), but unlike in the case of the two first ones, the capacitors are now implemented with interdigital structures, enabling a structure with only two metal layers and a single dielectric layer between them. The radiating loop is positioned diagonally and the top and ground metal layers are connected with a single 2 mm via at the both ends. The ground layer is all-metal.

Prototype 4), 30 mm * 22 mm * 2.3 mm in dimensions, is made by folding an etched inlay of PET (Mylar™) and aluminum around a brick of transparent polycarbonate. The matching network is of type c) and the only capacitor $C_p$ is realized with interdigital structures on the inlay. There is no galvanic contact between the ends of the inlay on the ground plane side of the transponder, but a large capacitance formed by the overlapping ends of the inlay.

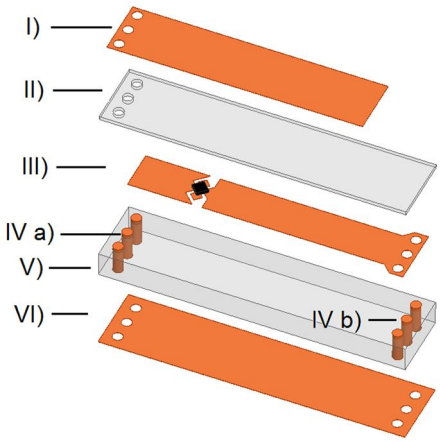


**Figure 3.** Exploded view of the transponder prototype 1).

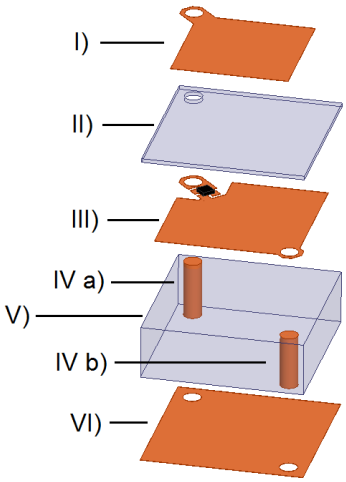


**Figure 4.** Exploded view of the transponder prototype 2).

## 4. Simulations and measurements

The electromagnetic simulations were done with Ansys High Frequency Structure Simulator (HFSS) 15 [7]. To simulate the operation of the transponder on a large metal object, the transponder was placed 0.5 mm above a copper plate of 230 mm × 230 mm that is large compared to the transponder, but still of practical size and not a multiple of half wavelengths that could excite resonance modes of the plate. In the simulations, the input impedance of each transponder type was optimized for the RF impedance of the microchip on the metal plate at the frequency of 867 MHz. The input impedance of the antenna as a function of frequency and the far field parameters including the radiation efficiency and the antenna directivity were recorded as the simulation results. Although the input impedance of the antenna was optimized for metallic mounting platform, the simulations were also made with the transponder model floating in free space, in order to evaluate the versatility of the transponders. The theoretical forward-link limited read range of the transponders can be then calculated from the simulation results by:

$$R_{read} = \frac{c}{2\omega}\sqrt{\frac{P_{tx\ EIRP} D_{tag} \eta_{tag}\left(1-\left|\frac{Z_{tag}-Z_{IC}^{*}}{Z_{tag}+Z_{IC}}\right|^{2}\right)}{P_{IC\ sens}}} \quad (1)$$

where $c$ is the speed of light, ω is the angular frequency, $P_{tx\ EIRP}$ is the equivalent isotropically radiated power of the reader device, $D_{tag}$ is the directivity of the transponder antenna, $\eta_{tag}$ is the radiation efficiency of the transponder antenna, $Z_{IC} = R_{cs} + jX_{cs}$ is the complex impedance of the microchip, $Z_{tag}$ is the input impedance of the transponder antenna and $P_{IC\ sens}$ is the read sensitivity of the microchip. '*' denotes complex conjugate. $P_{tx\ EIRP}$ = 3.28 W (2 W ERP), which is the maximum allowed radiated power of a UHF RFID reader as defined by ECC / ETSI [8]. The microchip used in the prototypes is Impinj Monza4, the impedance of which is $Z_{IC}$ = (13 – j151) Ω @ 867 MHz and sensitivity $P_{IC\ sens}$ = -17.4 dBm [9]

The prototypes were measured with Tagformance UHF RFID device using its own anechoic cabinet [10]. In the measurements, the transponder was attached with a piece of two-sided tape on a 230 mm × 230 mm sized 1 mm thick copper plate that is on a similar platform that was used in the simulations. The measurements were also made with the transponder in free space that is attached to a piece of Styrofoam in practice. The evaluation is based on measuring the activation level of the transponder as a function of frequency in a fixed and known setup, which is normalized for each measurement series with a standard transponder, the frequency response of which is known [11]. As a result, the measurement gives the equivalent forward-link limited read range that is directly comparable with the value calculated by (1) from the simulation results.

The simulated antenna parameters of the transponders at 867 MHz on metal are listed in Table 1. The simulated and measured forward-link based read ranges as a function of frequency are shown in Figures 5 – 8.

**Table 1.**
Simulated transponder parameters @ 867 MHz on metal.

| tag type | $Z_{tag}$ (Ω) $R$ | $X$ | $\eta_{tag}$ (%) | $D_{tag}$ (dBi) | $R_{read}$ (m) |
|---|---|---|---|---|---|
| 1) | 11 | 152 | 1.7 | 5.5 | 2.8 |
| 2) | 2.0 | 144 | 4.9 | 5.6 | 3.2 |
| 3) | 5.7 | 150 | 18 | 5.4 | 7.9 |
| 4) | 5.5 | 153 | 13 | 5.5 | 7.1 |

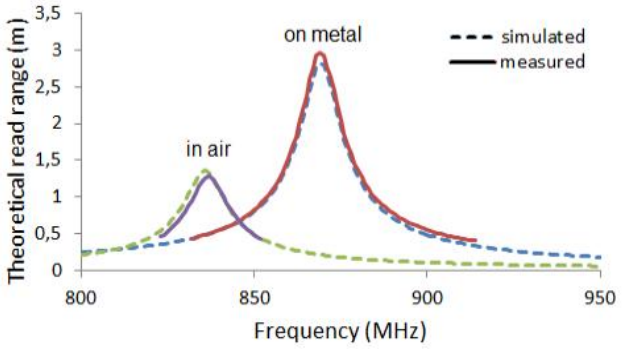


**Figure 5.** Theoretical read range of the prototype 1) as a function of frequency: simulation and measurement results compared on metal and in air.

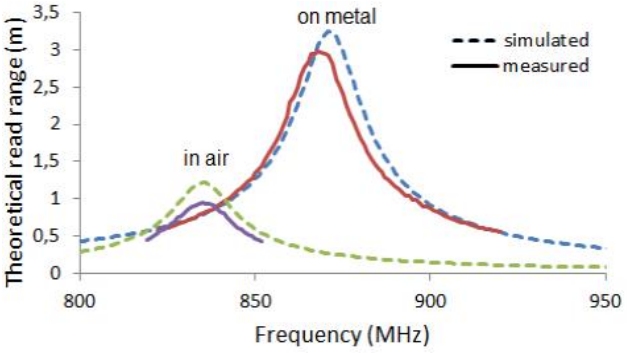


**Figure 6.** Theoretical read range of the prototype 2) as a function of frequency: simulation and measurement results compared on metal and in air.

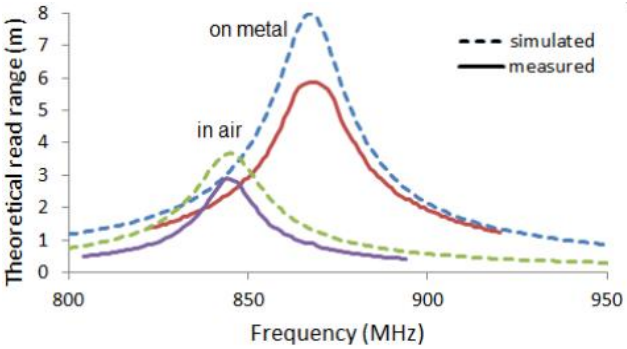


**Figure 7.** Theoretical read range of the prototype 3) as a function of frequency: simulation and measurement results compared on metal and in air.

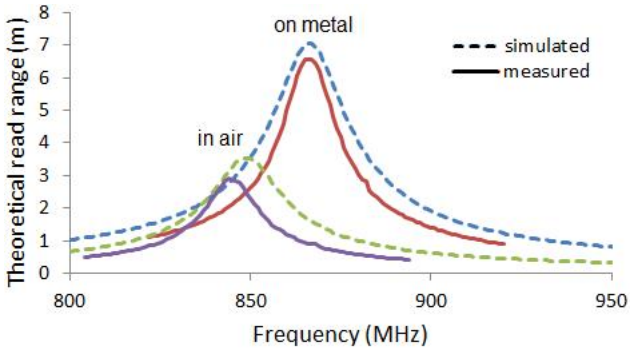


**Figure 8.** Theoretical read range of the prototype 4) as a function of frequency: simulation and measurement results compared on metal and in air.

## 5. Conclusion

Four types of small UHF RFID transponders were successfully demonstrated. The simulation and measurement results of the transponders appeared to be in fairly good agreement with each other; only the on-metal read range of type 3) remained more than slightly below the value predicted by the simulation. The results show the effect of impedance matching well; type 1), which by volume is the smallest of the prototypes, but the antenna of which is conjugately matched to the impedance of the microchip, has almost as long read range as type 2), although the radiation efficiency of type 1) is only one third of the value of type 2). On the other hand, type 2) has broader bandwidth due to its lower internal Q value, which is also an important feature considering fabrication tolerances. Bigger size of the transponder means bigger radiating loop and thus greater radiation efficiency and consequently longer read range. Table 1 shows that the read range of type 3) can be easily increased by about 8 % by adjusting its two capacitance values further for conjugate impedance match, if narrow bandwidth can be accepted. Equipping the tags with a more sensitive microchip, such as Impinj Monza R6, would increase the read range further by about 35 % [12].

## 6. Acknowledgements

The author would like to thank Mr. Yoshihiko Tsujimoto, CEO of AssetSmarty, for cooperation and for arranging the fabrication of the prototypes fabricated on PCB.

## 7. References

1. F. Fuschini, C. Piersanti, L. Sydanheimo, L. Ukkonen and G. Falciasecca, "Electromagnetic Analyses of Near Field UHF RFID Systems," *IEEE Transactions on Antennas and Propagation*, vol. 58 no. 5, May 2010, pp. 1759–1760.

2. S-L Chen, "A Miniature RFID Tag Antenna Design for Metallic Objects Application," *IEEE Antennas and Wireless Propagation Letters,* Vol. 8, 2009, pp. 1043 – 1045

3. T. Björninen, L. Sydänheimo, L. Ukkonen, and Y. Rahmat-Samii, "Advances in antenna designs for UHF RFID tags mountable on conductive items," *IEEE Antennas and Propagation Magazine*, vol. 56, no. 1, February 2014, pp. 79–103

4. K. Jaakkola, "Small On-metal UHF RFID Transponder with Long Read Range," *IEEE Transactions on Antennas and Propagation*, Vol. 64, no. 11, November 2016, pp. 4859 – 4867

5. W. Jillek and W. K. C. Yung, "Embedded components in printed circuit boards: A processing technology review," *Int. J. Adv. Manuf. Technol.*, vol. 25, no. 3, 2005, pp. 350–360

6. RO4000 Series High Frequency Circuit Materials by Rogers Corporation, accessed on Jan. 29th, 2017. [Online]. Available:https://www.rogerscorp.com/documents/726/acs/RO4000-LaminatesData-sheet.pdf

7. Ansys HFSS High Frequency Electromagnetic Field Simulation, accessed on Jan. 29th, 2017. [Online]. Available:http://www.ansys.com/Products/Electronics/ANSYS-HFSS

8. ERC Recommendation 70–03 Relating to the Use of Short Range Devices (SRD), p. 34, accessed on Jan. 29th , 2017. [Online]. Available: http://www.erodocdb.dk/docs/doc98/official/pdf/rec7003e.pdf

9. Impinj Monza4 UHF RFID Microchip, Datasheet, accessed on Jan. 29th, 2017. [Online]. Available: http://www.impinj.com/Documents/Tag_Chips/Monza_4_Tag_Chip_Datasheet/

10. Tagformance Pro by Voyantic, accessed on Jan. 29th, 2017. [Online]. Available: https://voyantic.com/products/tagformance-pro

11. P. Nikitin, K. V. S. Rao, and S. Lam, "UHF RFID Tag Characterization: Overview and State-of-the-Art," accessed on Jan. 29th, 2017. [Online]. Available:https://pdfs.semanticscholar.org/4c92/ad48e34cf7ef6a11e7652819cb6cb293d9e2.pdf

12. Impinj Monza R6™ UHF RFID microchip, datasheet, accessed on Jan. 29th, 2017. [Online]. Available: https://support.impinj.com/hc/en-us/articles/202765328-Monza-R6-Product-Datasheet